Hyperactive CREB subpopulations increase during therapy in pediatric B-lineage acute lymphoblastic leukemia

Dino Masic,[1] Kayleigh Fee,[2] Hayden L. Bell,[1] Marian Case,[1] Gabby Witherington,[1] Sophie Lansbury,[1] Juan Ojeda-Garcia,[3,4] David McDonald,[3,4] Claire Schwab,[1] Frederik W. van Delft,[1] Andrew Filby[3,4] and Julie Anne Elizabeth Irving[1]

[1]Wolfson Childhood Cancer Research Centre, Newcastle University Centre for Cancer, [2]Haematology Department, Flow Cytometry Laboratory, Royal Victoria Infirmary, [3]Newcastle University Flow Cytometry Core Facility, Newcastle University and [4]Innovation, Methodology and Application Research Theme, Newcastle University, Newcastle upon Tyne, UK

Correspondence: J. Irving
julie.irving@newcastle.ac.uk

Received: June 21, 2022.
Accepted: November 10, 2022.
Early view: November 24, 2022.

https://doi.org/10.3324/haematol.2022.281177

Abstract

Persistence of residual disease in acute lymphoblastic leukemia (ALL) during the initial stages of chemotherapy is associated with inferior survival. To better understand clonal evolution and mechanisms of chemoresistance, we used multiparameter mass cytometry, at single-cell resolution, to functionally characterize pediatric B-ALL cells at disease presentation and those persisting during induction therapy. Analysis of ALL cells from presentation samples (n=42) showed that the most abundant phosphosignals were pCREB, pH2AX and pHH3 and we identified JAK-STAT and RAS pathway activation in five of six patients with *JAK* or *RAS* genetic aberrations. The clonal composition of ALL was heterogeneous and dynamic during treatment but all viable cell clusters showed pCREB activation. Levels of pCREB in ALL cells were increased or maintained during therapy and high dimensional analysis revealed a subpopulation of ALL cells at presentation that was positive for pCREB/pHH3/pS6 which increased during treatment in some patients, implicating this signaling node in conferring a survival advantage to multi-agent induction therapy. The small molecule CREB inhibitor, 666-15, was shown to reduce CREB transcriptional activity and induce apoptosis in ALL patient-derived xenograft cells of varying cytogenetic subtypes *in vitro*, both in the presence and absence of stromal support. Together, these data suggest that the cAMP signaling pathway may provide an opportunity for minimal residual disease-directed therapy for many patients at high risk of relapse.

Introduction

Childhood acute lymphoblastic leukemia (ALL) is the most common childhood malignancy and while outcome has improved dramatically over the last 50 years, relapsed ALL remains a major cause of cancer death in children.[1,2] There are a number of well-recognized prognostic biomarkers at presentation of ALL including age, peripheral white blood cell count, morphology and key cytogenetic abnormalities.[3] However, the most powerful, independent prognostic factor is the response of the leukemia to initial chemotherapy.[4] Thus, levels of persisting leukemia cells assessed at 8, 15 or 28 days after the start of induction chemotherapy are highly prognostic. These are monitored initially by morphology, and subsequently by more sensitive methods to evaluate submicroscopic disease, known as minimal residual disease (MRD). Incorporation of residual disease assessment into contemporary trials has enabled risk-directed therapy and has been fundamental in children receiving personalized, optimal therapy.[5,6]

Genetic analyses of paired ALL samples at presentation and relapse have revealed a number of recurrent pathways implicated in relapse, including RAS, JAK-STAT, cell cycle and B-cell development, as well as genes involved in epigenetic modification.[7] Our own data, together with data from others, also implicate cell maturation as a resistance mechanism.[8,9] Genomic analyses have revealed extensive clonal diversity and, in most cases, leukemic cells at relapse are related to a major or minor clone of cells found at presentation that have survived therapy and acquired additional mutations to give rise to the relapse.[10-16] This selection of mutated clones has been noted in the early stages of treatment, when their proportion relative to the total leukemic burden increases during the selective pressure of multi-agent induction therapy.[14,17,18] Thus, the genotype, phenotype and therapeutic vulnerabilities of the leukemic clone persisting after induction chemo-

therapy may be very different from those at presentation. Drugs targeting MRD and mechanisms of chemoresistance may avert relapse.

MRD is routinely quantified by two different methodologies: molecular analyses of antigen receptor gene rearrangements and flow cytometry of aberrant immunophenotypes.[19] Flow MRD relies fundamentally on the characterization of a leukemia-associated immunophenotype (LAIP) at presentation, an antibody combination that discriminates leukemic cells from normal lymphocyte progenitors and can thus be used for 'on treatment' samples to discriminate and quantify ALL cells. An advantage of cytometric methods is that, as cell-based assays, they can provide information beyond that of just MRD quantitation, including the mechanism behind the evasion of chemotherapy-induced killing and the presence of therapeutic targets. In this study, we used single-cell, high-dimensional mass cytometry to functionally characterize pediatric B-ALL cells both at presentation and persisting during therapy. We demonstrated the presence of activated cAMP response element-binding protein (CREB) across a broad spectrum of cytogenetic groups at presentation and found minor subpopulations with hyperactive CREB at presentation that appeared to have a selective advantage during induction therapy. We also validated CREB as a therapeutic target in ALL cells using a specific inhibitor of CREB transcriptional function. CREB and its signaling pathway may provide an opportunity for MRD-directed therapy.

Methods

Clinical samples

Bone marrow samples from children with B-lineage ALL were accessed through the Newcastle Haematology Biobank, after appropriate consent (reference numbers 2002/111 and 07/H0906). All patients were registered on the ALL2003 or the UKALL2011 trials which used an induction regimen consisting of three or four drugs, depending on National Cancer Institute risk factors. MRD was assessed using a standardized flow cytometry method that was adapted from four to seven or eight colors.[20] The clinical details of the patients included in the study are listed in *Online Supplementary Tables S1* and *S2* and a CONSORT diagram is shown in *Online Supplementary Figure S1*.

Cell lines and patient-derived xenograft cells

ALL cell lines were obtained from the European Collection of Authenticated Cell Cultures (ECACC), maintained in RPMI-1640 (Sigma-Aldrich, Dorset, UK) supplemented with 10% fetal bovine serum (Gibco, Rugby, UK), and incubated at 37°C in a 5% CO_2 atmosphere. Patient-derived xenograft (PDX) cells were originally created by intrafemoral injection of presentation primary bone marrow samples into NOD SCID γ null mice, as described previously.[17] Clinical details of these grafts are also included in *Online Supplementary Table S1*.

Western blotting

Cells were washed in phosphate-buffered saline and proteins were extracted using PhosphoSafe extraction reagent (Merck, Nottingham, UK) supplemented with protease inhibitors (Roche, Hertfordshire, UK). Western blotting was carried out using a standard methodology with antibodies for pCREB (pS133), CREB, ERK2 (Santa Cruz, Dallas, TX, USA), p-p44/42 MAPK (Erk1/2) (Thr202/Tyr204), pSTAT5 (pT694), STAT5 (Cell Signaling Technology, Danvers, MA, USA) and α-tubulin (Sigma-Aldrich, St. Louis, MO, USA) which served as a loading control. Densitometry was carried out using AIDA image analysis software (Raytest, Straubenhardt, Germany).

Pharmacodynamic assays

Externalization of annexin V (Abcam, Cambridge, UK) was assessed by flow cytometry on a FACSCalibur (BD Biosciences, New Jersey, NJ, USA), fitted with a 488 nm laser. The CREB pathway was stimulated by dosing ALL cell lines with 50 μM forskolin and 100 μM IBMX diluted in dimethylsulfoxide for 30 minutes prior to treatment with 666-15. The mRNA levels of CREB gene targets that we had previously identified in ALL cells[21] were assessed by quantitative real-time polymerase chain reaction (RQ-PCR) analysis. We included primer probe sets (Invitrogen, Carlsbad, CA, USA) for *CXCR4* and *MKNK2*, with *TBP* used as a housekeeping control, as described previously.[21]

Statistical analyses

All statistical analyses were performed using Graphpad Prism. A *P* value of less than 0.05 was considered statistically significant.

Additional methods are provided in the *Online Supplementary Material*.

Results

Mass cytometry analyses of presentation B-acute lymphoblastic leukemia samples revealed prominent pCREB/ATF1 signaling and identified JAK-STAT and RAS pathway activated leukemia

Mass cytometric analyses of B-lineage ALL at presentation (n=42) was performed; live, singlet, non-apoptotic ALL cells were gated by their specific LAIP and mature B cells were identified by the immunophenotype $CD34^-/CD10^-/CD22^+/CD45^+$. The normalized mean mass intensity (MMI) of all phospho-antibodies in the ALL cells, relative to mature B cells, is shown in Figure 1A. The most prominent phospho-signals were pCREB/pATF1 [S133] (median, 23.95;

range, -37.52 to 141.2), pH2AX [S139] (median, 7.53; range, -10.81 to 79.24) which is a marker of double-strand breaks, and pHH3 [Ser28] (median, -2.49; range, -107.1 to 71.5) which is activated in cells undergoing mitosis.

For ALL cases at presentation for which there was sufficient stored material, we performed western blot analyses to validate our mass cytometry findings. Western blotting showed high expression of CREB in all ALL cells and confirmed the variable activation of both CREB and its close family member, ATF1 (activating transcription factor 1) (Figure 1B). Western blot analyses for pSTAT5 [Y694] showed that three of seven samples were positive and these had the highest MMI values (Figure 2A, *Online Supplementary Figure S2*). All three positive samples were B-other ALL, one with a *PAX5-JAK2* and another with an *IGH-CRLF2* translocation. With regard to pERK, three of seven samples were positive by western blot analyses and two of the positive samples had the highest pERK MMI in the group. These two samples were also B-other ALL, one of which had a known *KRAS* mutation.

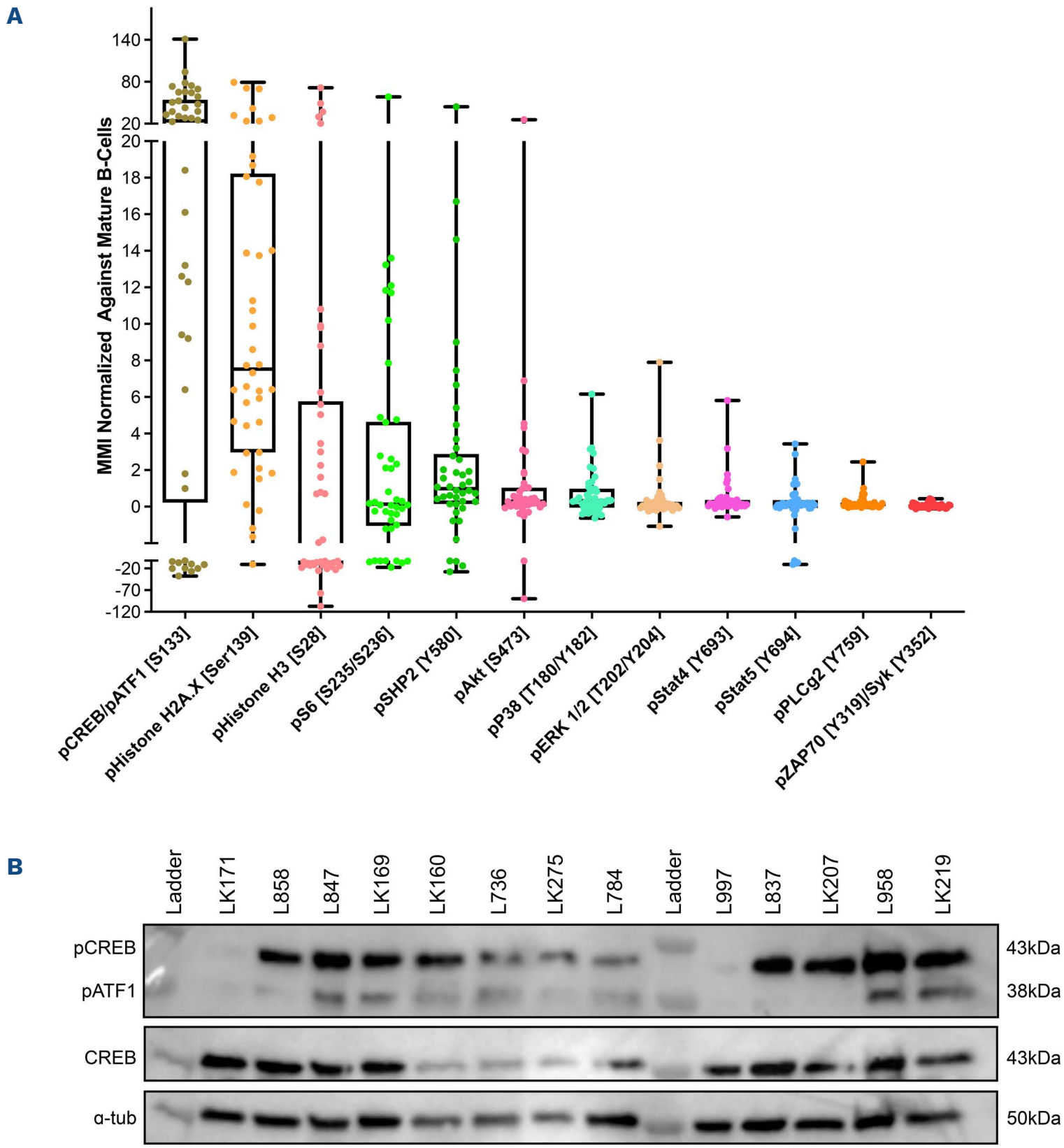

Figure 1. pCREB/pATF1 [S133] is heterogeneously expressed in acute lymphoblastic leukemia at presentation. (A) Box and whisker plot of normalized phospho-signals showing median, upper and lower quartiles and range in acute lymphoblastic leukemia (ALL) samples at presentation normalized to the signals of mature B cells, as detected by mass cytometry. (B) Western blot analysis of ALL lysates for pCREB/ATF1 [S133], CREB and α-tubulin in a representative set of presentation ALL samples that were typical of the cohort.

When the cases of ALL were grouped by cytogenetic risk, levels of pSTAT5 MMI were lower in the good-risk cytogenetic group compared to the intermediate- and poor-risk groups, with means of -2.24 *versus* 0.48 *versus* 0.36, respectively (P<0.005) (Figures 2B). There was also a trend for higher pHH3 [Ser28] and pCREB/pATF1 [S133] levels with increasing cytogenetic risk, but the differences did not achieve statistical significance (P=0.067 and P=0.29, respectively) (Figure 2C, D).

Residual disease cells show maturation and increased phospho-signaling in pHH3 and pCREB

MMI for antigens were again normalized to mature B cells within each sample and values compared between presentation samples (n=42) and MRD samples (n=15 in total; n=5 at day 8, n=8 at day 28 and n=2 at later time points), identified by sequential gating (Table 1A, *Online Supplementary Figure S3*). MRD levels determined by flow or mass cytometry were highly concordant in this cohort and a pilot cohort (*Online Supplementary Figure S4*). Compared to presentation ALL cells, MRD showed a significant increase in the expression of the cell surface antigens, CD45 (P<0.01) and CD22 (P<0.05), and a trend to an increase in CD19 (P=0.078), consistent with maturation as previously reported.[8] There was also a highly significant increase in the level of pHH3 (P<0.001), from a MMI of -3.14 in presentation ALL cells to 62.48 in MRD cells. pCREB levels increased from 26.70 to 69.85 (P<0.01). There were also more modest increases in pp38, pSTAT5 and pZAP70 and a decrease in pSHP2 (P<0.05). In paired presentation and MRD samples (n=10), the same trends in antigen expression were observed but only the increase in pHH3 remained statistically significant (P<0.05) (Table 1B). A decrease of CD10 levels in MRD cells also gained signifi-

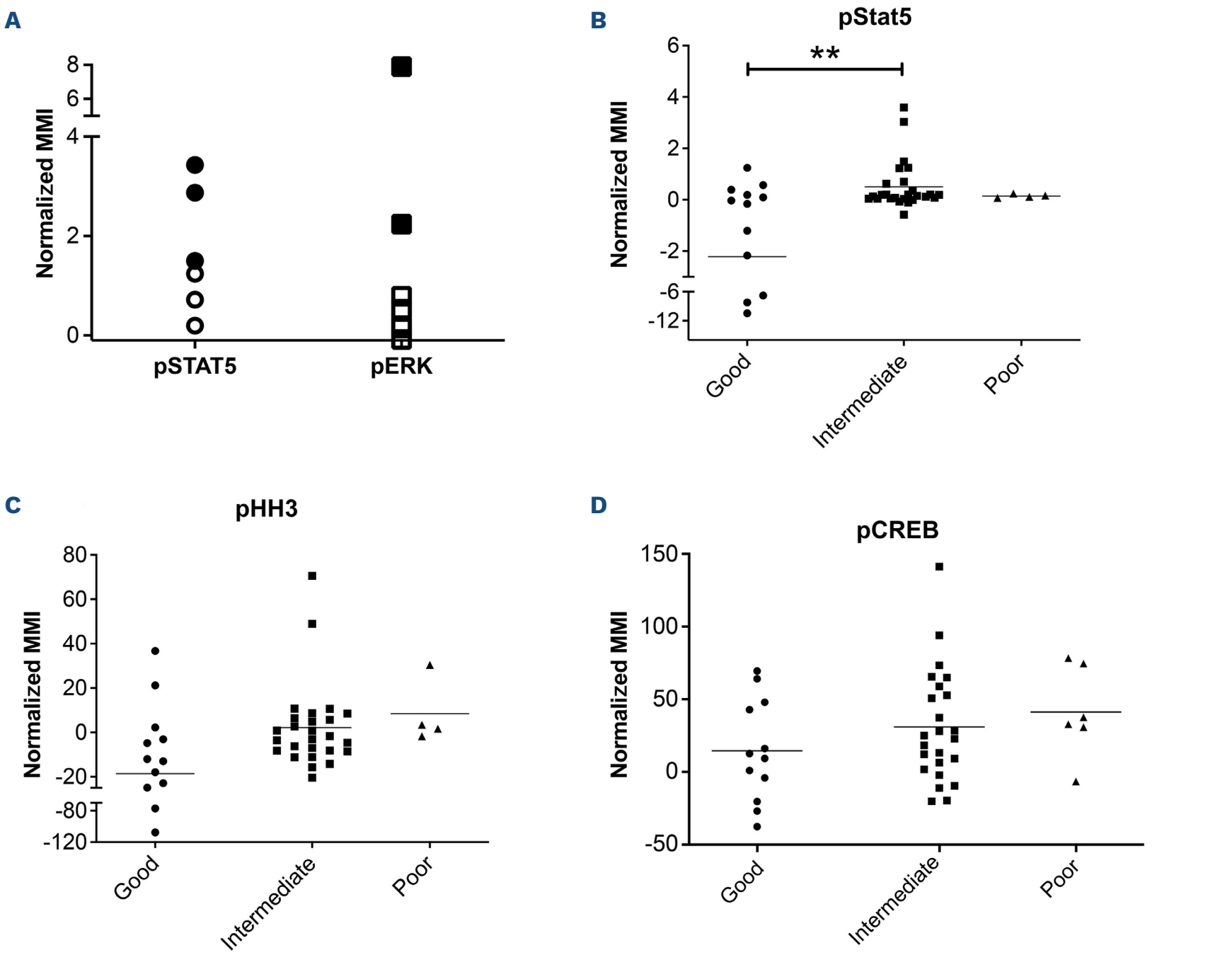

Figure 2. Phospho-signals determined by mass cytometry identify JAK-STAT and RAS pathway activation and a correlation of pSTAT5 activation with cytogenetic risk. (A) Normalized mean mass intensity (MMI) for pSTAT5 and pERK in presentation samples of acute lymphoblastic leukemia (ALL) with pathway activation assessed by both mass cytometry and western blot analysis. Solid black shapes denote ALL samples that are positive by western blot analysis. (B-D) Normalized MMI in good-, intermediate- and poor-risk cytogenetic groups for pSTAT5 (B), pHH3 (C) and pCREB (D). $^{**}P$<0.01.

cance (P<0.05) There was no difference in MMI values in mature B cells in samples taken at presentation or while on treatment, validating their reliability as an internal control (*Online Supplementary Table S3*).

The clonal composition of acute lymphoblastic leukemia is dynamic during therapy but all clusters have activated pCREB and high pCREB subpopulations in minimal residual disease are often enriched during induction therapy

To investigate the clonal composition of ALL cells during therapy, we used FlowSOM as part of the R Studio CyTOF workflow package to perform cluster analyses of ALL cells in paired presentation and MRD samples using only phospho-signals and identified 20 unique ALL cell clusters. Most ALL were complex and heterogeneous, showing multiple different clusters at both presentation and in MRD and clonal composition was dynamic during therapy (Figure 3). Despite the varying cytogenetics of the cohort, eight clusters made up more than 94% of the total cluster composition (Figure 4A). All clusters showed expression of pCREB, except clusters 6 and 7 which had very low expression of pHH3 and high levels of pH2AX and were, therefore, likely to be damaged cells that had not yet expressed the apoptotic markers that would have ensured their being gated out from the analyses. One cluster, cluster 10, was significantly more prevalent in MRD cells than in presentation, drug-naïve ALL cells (P<0.05) and was characterized by high levels of pCREB, pHH3 and pS6 (Figure 4B, C). We used the dimension reduction algorithm, Uniform Manifold Approximation and Projection (UMAP) to compare ALL cell clusters at presentation and at MRD. UMAP plots displayed one dominant island comprising the majority of generated clusters and showed an area populated only by presentation ALL at the top left of the plot, housing cluster 11, and two areas at the bottom populated predominantly by MRD (clusters 10, 15 and 16) but most areas having both (both clusters 3, 4 and 14) (Figure 5A, B). Two additional minor islands were generated: one was characterized by pSHP2 expression and comprised clusters 1, 2 and 8, the other expressed pH2AX and comprised clusters 6, 7, 9, and 17 (*data not shown*). Visualization of pCREB confirmed its ubiquitous ex-

Table 1. Mean mass intensity of acute lymphoblastic leukemia cells, normalized to mature B cells, in (A) unpaired and (B) paired samples taken at presentation and during treatment.

A					
	Presentation		MRD		
Antigen	MMI	Range	MMI	Range	*P* value
pp38	0.74	6.78	2.73	25.90	**0.034***
pAKT	-0.77	115.35	1.20	21.66	0.61
pCREB	26.70	178.72	69.85	281.80	**0.004****
pERK	0.45	8.15	0.38	2.33	0.85
pHH3	-3.14	178.60	62.48	246.49	**0.00*****
pPLCg2	0.22	2.50	0.21	0.81	0.89
pS6	2.71	76.02	4.93	40.27	0.49
pSHP2	2.69	58.00	-2.94	30.44	**0.022***
pSTAT4	0.49	5.91	1.02	8.23	0.21
pSTAT5	-0.32	14.10	1.65	12.60	0.019*
pZAP70	0.07	0.54	0.38	3.12	0.015*
pH2AX	14.66	90.05	6.46	60.87	0.16
CD10	49.47	183.61	33.47	119.83	0.21
CD45	-237.34	520.70	-101.02	406.49	**0.003****
CD38	74.48	295.45	47.89	277.39	0.24
CD22	-110.62	370.10	-55.33	199.50	**0.013***
CD123	21.02	144.11	35.43	158.89	0.20
CD34	25.19	141.89	24.95	78.19	0.98
CD19	-73.96	446.00	-5.08	614.66	**0.078**
CD58	16.63	98.51	21.30	66.51	0.43

B					
	Presentation		MRD		
Antigen	MMI	Range	MMI	Range	*P* value
pp38	0.90	6.78	1.93	25.90	0.57
pAKT	1.03	4.83	1.30	21.66	0.87
pCREB	42.40	114.30	67.11	253.70	0.30
pERK	1.39	8.10	0.30	2.33	0.14
pHH3	-2.70	54.80	56.38	243.10	**0.014***
pPLCg2	0.22	0.77	0.16	0.49	0.40
pS6	1.44	10.21	5.01	40.27	0.33
pSHP2	1.53	28.26	-2.58	35.22	0.22
pSTAT4	1.15	5.91	1.00	8.43	0.86
pSTAT5	-0.01	14.10	1.50	12.60	0.32
pZAP70	0.13	0.53	0.37	3.15	0.38
pH2AX	5.85	30.87	2.08	23.27	0.21
CD10	54.12	110.14	28.22	61.40	**0.042***
CD45	-171.36	236.40	-87.60	406.49	0.08
CD38	52.91	135.83	56.27	277.39	0.90
CD22	-83.23	135.86	-46.85	199.50	0.09
CD123	54.27	135.26	40.64	155.05	0.50
CD34	25.17	50.88	22.11	47.89	0.65
CD19	-21.20	196.20	20.63	609.95	0.41
CD58	16.15	45.39	22.11	66.51	0.42

The mean mass intensity (MMI), its range and the statistical significance of differences between values for pre-treatment (presentation) samples of acute lymphoblastic leukemia (ALL) cells and those during treatment (with minimal residual disease, MRD). (A) An unpaired, two-tailed, equal variance *t* test was performed on presentation *versus* MRD ALL MMI signals. (B) A paired, two-tailed, equal variance *t* test was performed on presentation *versus* MRD ALL MMI signals. Statistically significant differences are shown in bold. *P<0.05, **P<0.01 and ***P<0.001.

pression across the UMAP in both presentation and MRD ALL cells, while pHH3 was more defined and concentrated in the MRD samples (Figure 5C, D). The MRD-enriched areas housed clusters 10, 15 and 16, which are characterized by high pCREB and pHH3. In samples for which there were sufficient MRD cells, individual UMAP showed that in five of seven patients, ALL cells with the highest pCREB levels were enriched during therapy, with pCREB levels often increasing further (Figure 6).

To investigate the effect of drugs on pCREB activation, we treated PreB 697 cells with the half maximal inhibitory concentration (IC_{50}) of the induction drugs, dexamethasone (67 nM) and vincristine (8.9 nM) on the CREB gene targets, *CCRX4* and *MKNK2* at various time-points. We

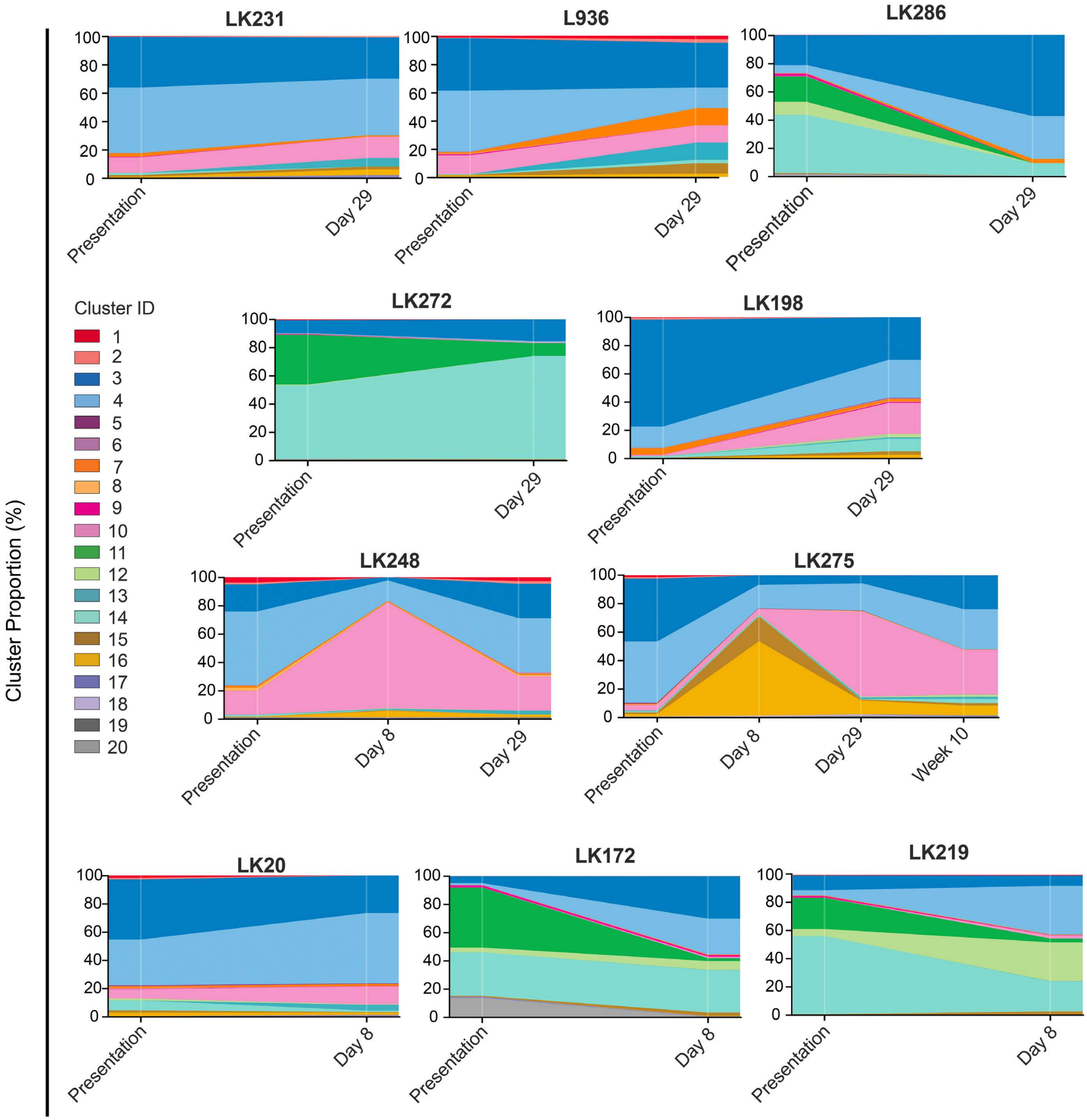

Figure 3. The clonal composition of acute lymphoblastic leukemia cells is complex and dynamic during therapy. Stacked bar plots show the percentages of clusters within acute lymphoblastic leukemia cells at presentation and at various time-points during treatment.

documented a modest induction of CCRX4 mRNA levels at the 3-hour time-point after dexamethasone dosing (P<0.01) (*Online Supplementary Figure S5*).

CREB inhibitors are cytotoxic in acute lymphoblastic leukemia

Since cluster analyses showed pCREB in all clusters of ALL cells, and identified a signaling node involving pCREB/pHH3/pS6 that is enriched in MRD, we sought to evaluate pCREB as a therapeutic target. We therefore dosed ALL cells with varying concentrations of 666-15, a potent, selective CREB inhibitor, and assessed cell viability relative to that of cells treated with the vehicle control. ALL cell lines (n=3) and PDX cells (n=3) grown in suspension culture were assessed using a metabolic readout and primary (n=10) and PDX cells (n=3), supported on a layer of mesenchymal stromal cells, were analyzed using high throughput imaging microscopy which yielded absolute cell numbers of both ALL blasts and mesenchymal stromal cells. IC_{50} values for cell lines ranged from 1.7 to 2.7 μM (mean, 2.4 μM), while those for primary/PDX cells ranged from 0.45 to 7 μM (mean, 2.6 μM) (Figure 7A, B). There was no difference in IC_{50} values of the three PDX samples grown in both suspension and on mesenchymal stromal support (P>0.75). There was no apparent correlation between levels of pCREB as assessed by western blot analysis and IC_{50} values (n=8, *data not shown*). Treating ALL cells with IC_{50} values of 666-15 was associated with induction of apoptosis as determined by phosphatidylserine externalization, with this effect being particularly marked in the PDX cells (P<0.05, paired *t* test) (Figure 7C). Pharmacodynamic experiments showed significant inhibition of *CXCR4* (n=4) (P=0.013) and *MKNK2* (n=4) (P=0.033) gene expression (Figure 7D, E), confirming on- target inhibition of CREB activity at the IC_{50} values for 666-15.

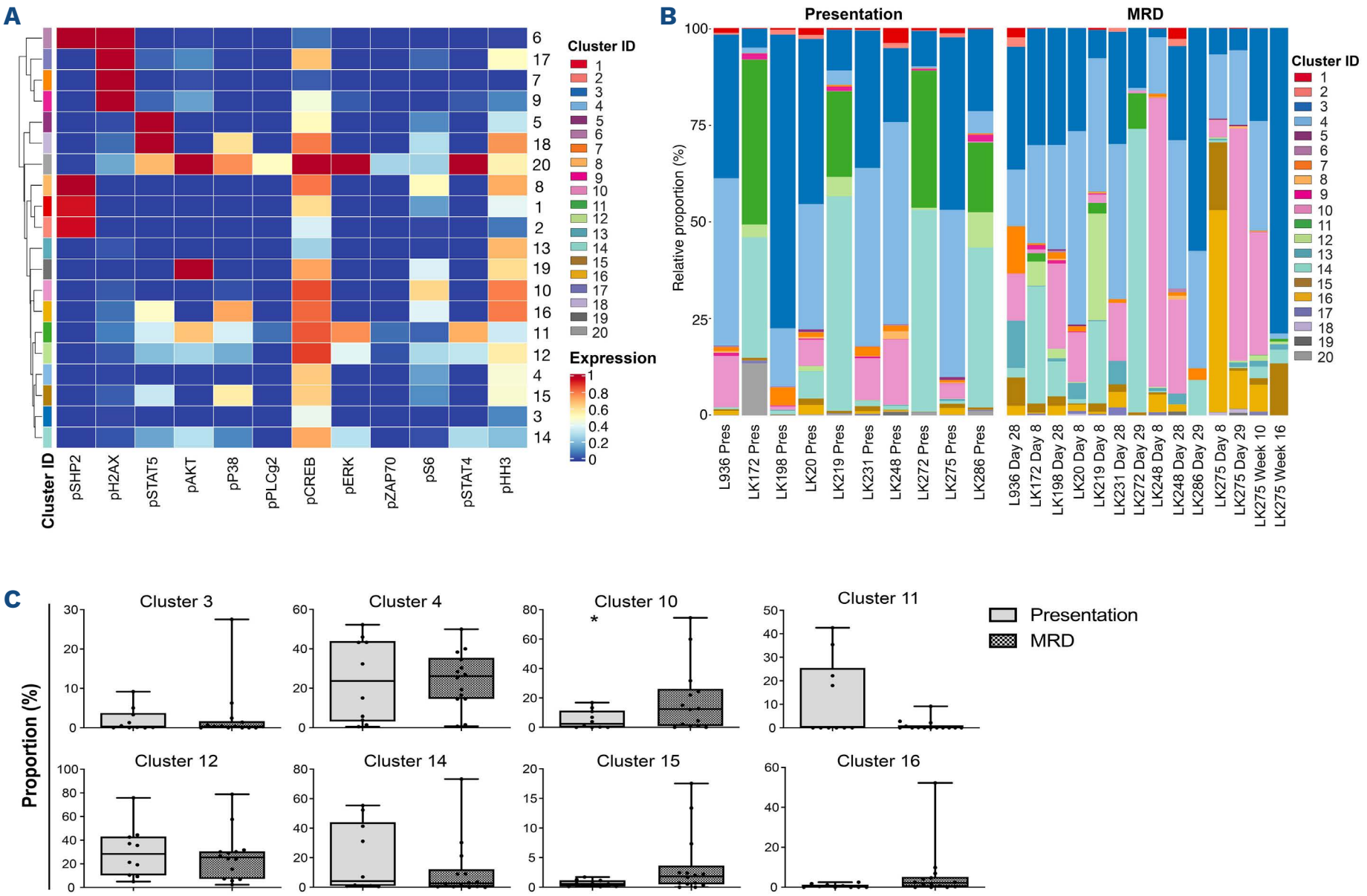

Figure 4. Cluster analysis revealed that phosphorylation of acute lymphoblastic leukemia cells at presentation (drug-naïve) and during treatment (with minimal residual disease) is complex and heterogeneous with all clusters having activated CREB and a cluster characterized by high levels of pCREB, pHH3 and pS6 having an apparent selective advantage during induction therapy. (A) Heatmap showing expression of target markers within generated clusters, with marker expression intensity displayed from low (blue) to high (red). (B) Bar chart showing whole population cluster composition within patients, separated into presentation and minimal residual disease (MRD) samples. (C) Box plots comparing the incidence of the top eight expressed clusters in the cohort of patients, comparing proportions of presentation and MRD samples of acute lymphoblastic leukemia (ALL) cells in the various clusters. *P<0.05.

Discussion

The extensive panel of antibodies used in this mass cytometric analysis adds a new diagnostic, functional dimension for ALL. Normal B cells and ALL cells can be identified prior to and during therapy. Functional parameters such as proliferation, apoptosis, pathway activation and quantification of key antigens were assessed in ALL cells and compared to those of normal B cells within the same sample. Thus in one assay, therapeutically relevant antibody targets, including CD19, CD22 and CD38 and signaling pathways, such as the JAK-STAT and the RAS pathways, can be assessed at the single-cell level. Importantly, this data-rich assay can be performed in samples with high or low leukemic burden. Thus for children with a poor response to induction or reinduction chemotherapy and at high risk of relapse, mass cytometry analysis could evaluate a range of predictive biomarkers to select the optimal targeted therapy directed at residual disease.

In our panel of presentation samples, levels of phosphorylated STAT5 were higher in the intermediate cytogenetic risk group than in the good-risk group, which is likely due to the high incidence of JAK-STAT genetic aberrations reported in Philadelphia chromosome-like and B-other sub-

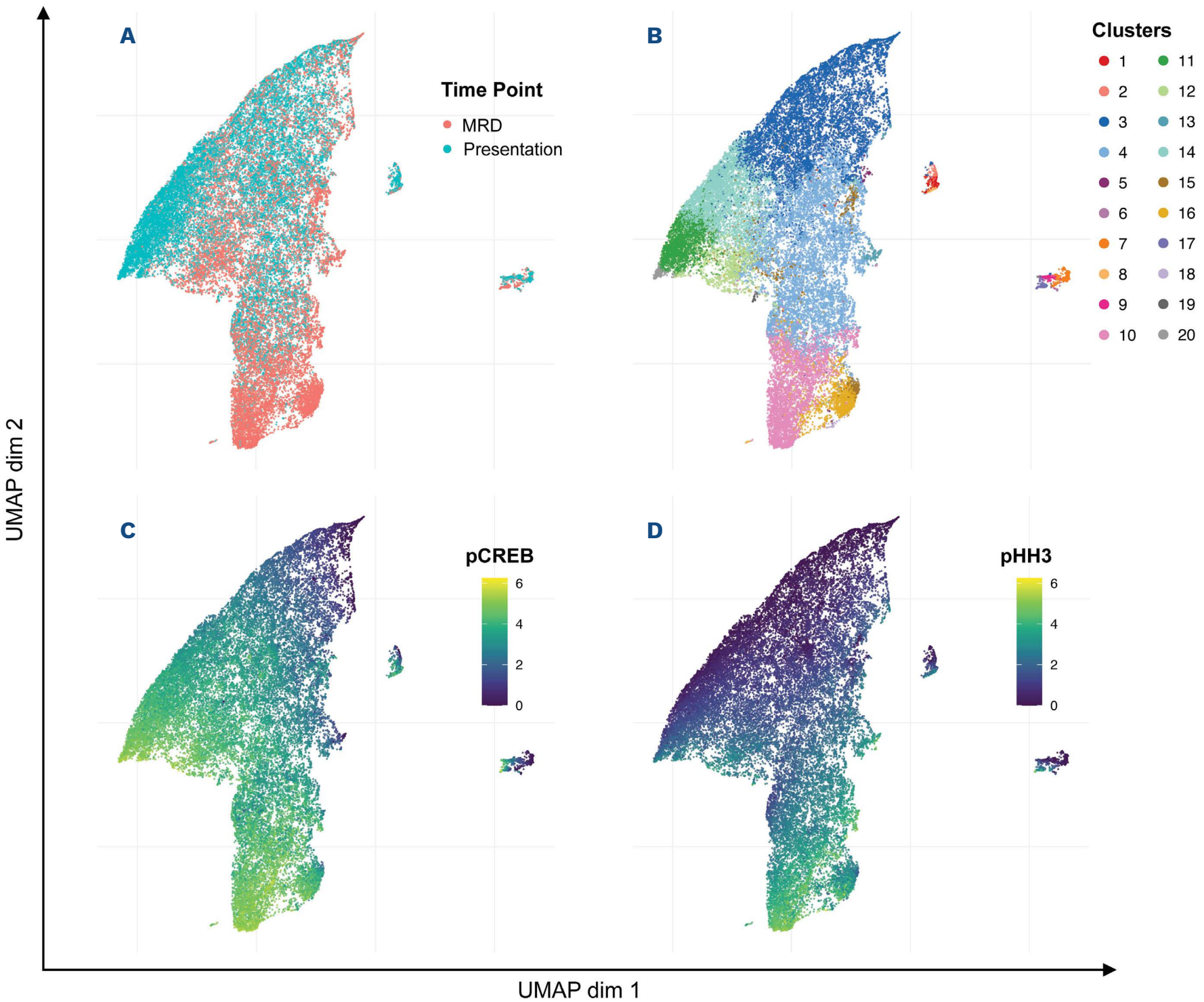

Figure 5. Uniform manifold approximation and projection analyses showing enrichment of clusters high in pCREB and pHH3 in minimal residual disease samples. Uniform manifold approximation and projection (UMAP) visualization of all analyzed cells shows variation between presentation and minimal residual disease (MRD) samples. (A) The distribution of presentation and MRD blasts shows a focus of MRD blasts to the south of the figure. (B) UMAP analysis showing the distribution of generated clusters in presentation and MRD blasts, with enrichment of clusters 10, 15, and 16 observed in the MRD blasts. (C) UMAP analysis showing pCREB levels in presentation and MRD blasts, with greater expression observed in MRD-enriched areas. (D) UMAP analysis showing the distribution of pHH3 in presentation and MRD blasts with a focus of pHH3 expression observed in MRD cells.

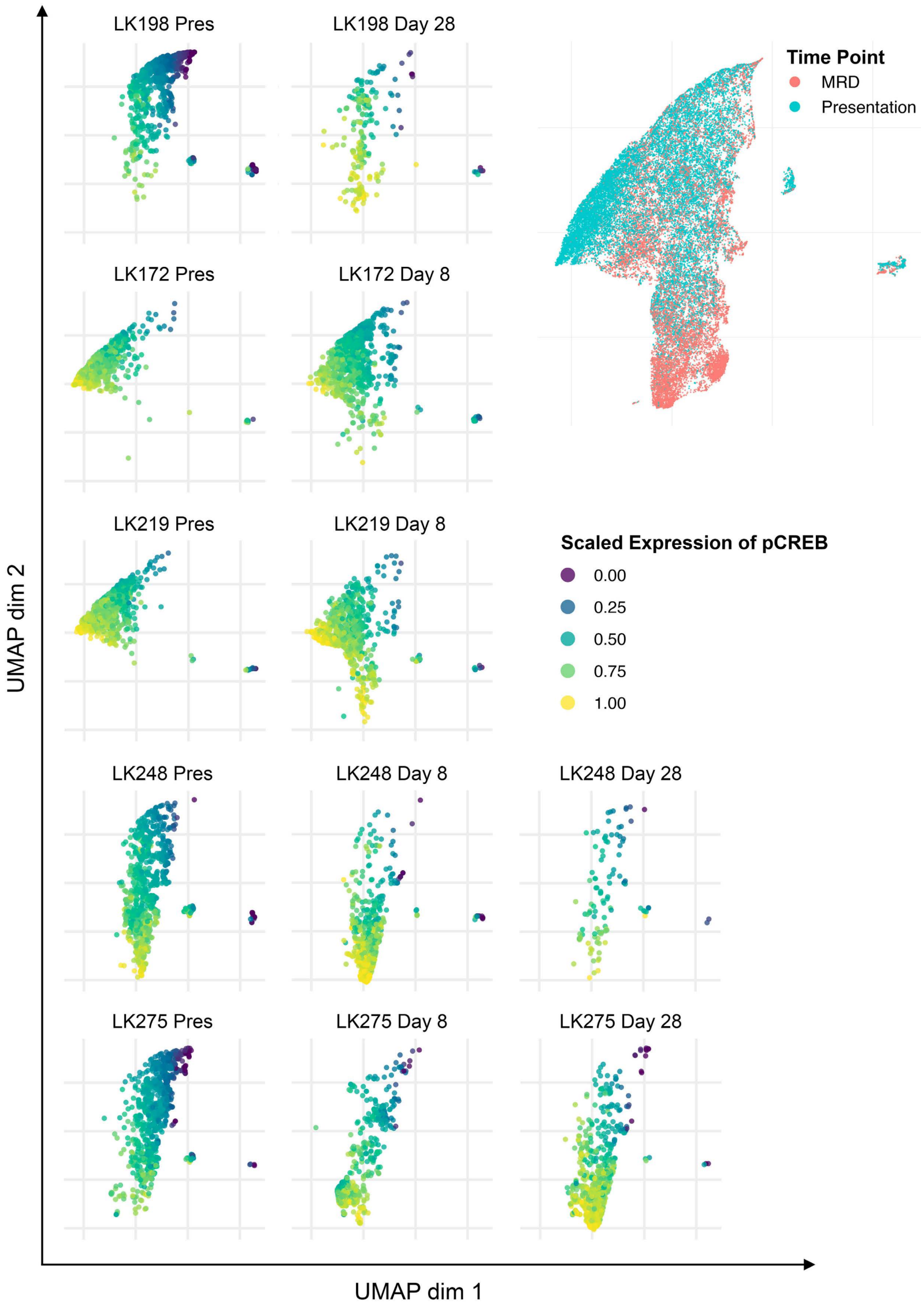

Figure 6. Uniform manifold approximation and projection analysis of individual patients show selection of high pCREB cells during induction therapy. The same uniform manifold approximation and projection (UMAP) as in Figure 5 but with visualization of pCREB levels in presentation and minimal residual disease (MRD) blasts in individual patients.

groups of ALL.[22] The high pSTAT5 and pERK levels were confirmed by western blotting and were often attributable to genetic aberrations known to activate these pathways and may serve as predictive biomarkers for sensitivity to JAK and MEK inhibitors.[17,23] Our data also confirmed the more mature immunophenotype of MRD cells compared to that of cells at presentation,[8,9] which suggests that anti-CD22 and anti-CD19 therapies such as inotuzumab and chimeric antigen receptor-modified T cells may be optimal at the end of induction when expression of antigens associated with B-cell maturation may be higher. We also identified a tendency for the levels of phosphorylated histone H3 (pHH3), a typical marker of mitotic cells, to be lower in good-risk cytogenetic ALL than in intermediate- and poor-risk groups. Phosphorylation of histone H3 at either Ser28 or Ser10 is a well-recognized prognostic biomarker in many cancer types but has not been explored in ALL.[24] Our data suggest that pHH3 may have a role in prognostic classification in ALL.

A major novel finding stemming from our data is the demonstration of high expression of activated CREB as a common feature of ALL, its increase in MRD cells and the demonstration that this increase is commonly due to hyperactive pCREB/pHH3 subpopulations increasing during induction treatment and persisting in MRD. This demonstrates a possible selective advantage of ALL clones that have high pCREB/pHH3/pS6 signaling under chemotherapeutic pressure. Further investigations will be needed to decipher whether this signaling node represents cells in G_2M or cells in interphase that have a small fraction of nucleosomes phosphorylated at Ser28 of HH3, related to transcriptional activities.[25] Other studies have suggested that MRD cells are in fact dormant.[26] Interestingly, our CREB data are supported by a small focused study in

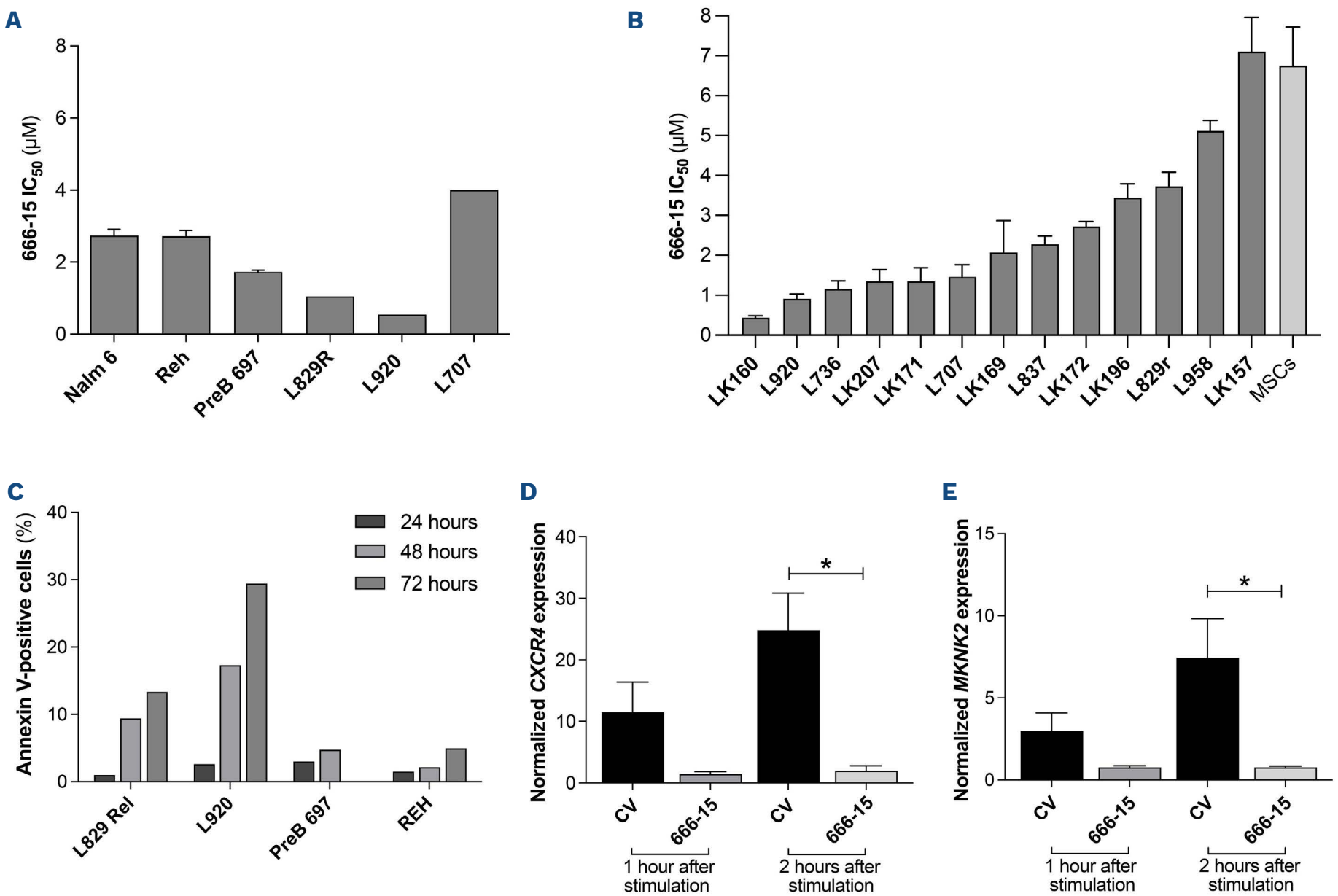

Figure 7. The CREB inhibitor, 666-15, is cytotoxic in acute lymphoblastic leukemia cells. (A) The half maximal inhibitory concentration (IC_{50}) of 666-15 for acute lymphoblastic leukemia (ALL) cell lines and patient-derived xenograft (PDX) ALL cells determined using an Alamar blue assay. The mean and standard error of mean (SEM) of three independent replicate experiments are shown for the cells lines. PDX are technical triplicates. (B) IC_{50} of 666-15 for primary and PDX ALL cells using mesenchymal stromal cell support. (C) Histogram showing the percentages of annexin V-positive cells after exposure to the specific IC_{50} of 666-15 for two PDX and two ALL cell lines after 24, 48 and 72 hours of incubation, normalized to that for the vehicle control. (D, E) Histogram of *CXCR4* (n=4) (D) and *MKNK2* (n=4) (E) gene expression in PreB697 cells after stimulation with forskolin and IBMX and subsequent dosing with the IC_{50} (1.7 µM) of 666-15 or control vehicle (CV) for 1 and 2 hours. The mean and SEM are shown. $^*P<0.05$.

CRLF2-positive ALL which also showed activation of pCREB at presentation, increased activation in MRD cells and a strong connection between pCREB and pS6.[27] Our study is the first to demonstrate this finding in a range of high-risk subtypes of ALL.

CREB and ATF1, along with cAMP response element modulator (CREM), are transcription factors of the basic leucine zipper superfamily which regulate gene expression through the activation of cAMP-dependent or -independent signal transduction. They can homo- or heterodimerize to bind cAMP response elements in target gene promoters. They are phosphorylated and activated by upstream serine-threonine kinases which increase their affinity to a number of transcriptional co-activators, including CREB-binding protein (CBP), p300 and transducers of regulated CREB (TORC). Phosphorylation of CREB at Ser133 is essential for CREB-mediated transcription and target gene function in cell proliferation, differentiation and survival. Overexpression and/or overactivation of CREB has been described in many types of cancer and phosphorylation of CREB at Ser133 can be catalyzed by a variety of kinases, including calcium/calmodulin-dependent (Cam) kinases that are activated by calcium fluxes, Akt or p90Rsk which are downstream of ERK, as well as protein kinase A, which is activated by cAMP. Functional analyses suggest that overexpression of CREB contributes to ALL cell proliferation and survival through transcriptional activation of gene targets involved in glycolysis and anti-apoptosis, including Bcl-2, Bcl-xL, Mcl-1 and survivin.[28-30] This array of anti-apoptotic CREB targets may explain the observed resistance to multi-agent induction chemotherapy. The importance of CREB in influencing clinical response has also been demonstrated in a study of adult ALL in which high levels of CREB and pCREB were associated with a shorter median overall survival; a similar trend was observed in pediatric disease.[30] Furthermore, a recent study identified expanded leukemic cell populations that, if present at the diagnosis of ALL, were associated with relapse.[31] One of the features of these expanded populations was high pCREB, again consistent with this pathway contributing to a chemoresistant phenotype.

Given their deregulation in many cancer types, CREB and CREB-specific signaling pathways have been proposed as targets for therapeutic intervention in cancer and inhibitors are being developed and have begun to enter early phase clinical trials.[32] Despite the universal role of CREB signaling in cells, pharmacological inhibition appears well-tolerated, both in preclinical models and according to data emerging from the clinic. This tolerance may be due to cancer cells being differently dependent on CREB activity as compared to their normal counterparts.[33] Thus, we preclinically evaluated a novel, specific small molecule CREB inhibitor in pCREB-positive ALL. 666-15 is a potent, selective inhibitor of CREB-mediated gene transcription, with an IC_{50} of 0.08 μM in cell-free assays. In a xenograft mouse model of breast cancer, it potently inhibited tumor growth, without overt toxicity and blood counts, blood chemistry, and tissue histology from liver, kidney and heart appeared similar to those of controls.[34] Our data from cell lines and PDX ALL cells showed that these were sensitive to concentrations of 666-15 that were achievable in mice and that the CREB inhibitor induced robust apoptosis in PDX ALL cells, consistent with a cytotoxic action. Inhibition of CREB transcriptional activity was clearly demonstrated at these cytotoxic concentrations.

In summary, we have established and validated a one-stop single-cell assay that can identify antigenic and signaling pathway targets in B-lineage ALL cells at both presentation of the disease and in 'on treatment' samples with high MRD. We show a role of hyperactive CREB, associated with an increase in subpopulations found in presentation samples, which appear preferentially selected for during induction therapy, suggesting that this pathway is involved in conferring chemoresistance to multidrug induction therapy. We propose that novel drugs affecting CREB activity or key downstream targets may be promising MRD-directed therapies for the majority of ALL patients at high risk of relapse.

Disclosures

JAEI has been awarded grant funding from Hoffmann La-Roche on an unrelated project. The other authors declare that they have no conflicts of interest to disclose.

Contributions

DM, HLB, KF, SL, GW, MC, DM, and CS performed research. CS, FWvD, HB, DM, JO-G, AF, and JAEI analyzed data. DM and JAEI wrote the manuscript. JAEI gained funding and supervised the study.

Data-sharing statement

Data are available on request.

References

1. Hof J, Krentz S, van Schewick C, et al. Mutations and deletions of the TP53 gene predict nonresponse to treatment and poor outcome in first relapse of childhood acute lymphoblastic leukemia. J Clin Oncol. 2011;29(23):3185-3193.
2. Parker C, Waters R, Leighton C, et al. Effect of mitoxantrone on outcome of children with first relapse of acute lymphoblastic leukaemia (ALL R3): an open-label randomised trial. Lancet. 2010;376(9757):2009-2017.
3. Pui CH, Carroll WL, Meshinchi S, Arceci RJ. Biology, risk stratification, and therapy of pediatric acute leukemias: an

update. J Clin Oncol. 2011;29(5):551-565.
4. Campana D. Minimal residual disease monitoring in childhood acute lymphoblastic leukemia. Curr Opin Hematol. 2012;19(4):313-318.
5. Vora A, Goulden N, Mitchell C, et al. Augmented post-remission therapy for a minimal residual disease-defined high-risk subgroup of children and young people with clinical standard-risk and intermediate-risk acute lymphoblastic leukaemia (UKALL 2003): a randomised controlled trial. Lancet Oncol. 2014;15(8):809-818.
6. Vora A, Goulden N, Wade R, et al. Treatment reduction for children and young adults with low-risk acute lymphoblastic leukaemia defined by minimal residual disease (UKALL 2003): a randomised controlled trial. Lancet Oncol. 2013;14(3):199-209.
7. Irving JA. Towards an understanding of the biology and targeted treatment of paediatric relapsed acute lymphoblastic leukaemia. Br J Haematol. 2016;172(5):655-666.
8. Dworzak MN, Schumich A, Printz D, et al. CD20 up-regulation in pediatric B-cell precursor acute lymphoblastic leukemia during induction treatment: setting the stage for anti-CD20 directed immunotherapy. Blood. 2008;112(10):3982-3988.
9. Nicholson L, Evans CA, Matheson E, et al. Quantitative proteomic analysis reveals maturation as a mechanism underlying glucocorticoid resistance in B lineage ALL and re-sensitization by JNK inhibition. Br J Haematol. 2015;171(4):595-605.
10. Anderson K, Lutz C, van Delft FW, et al. Genetic variegation of clonal architecture and propagating cells in leukaemia. Nature. 2011;469(7330):356-361.
11. Davidsson J, Paulsson K, Lindgren D, et al. Relapsed childhood high hyperdiploid acute lymphoblastic leukemia: presence of preleukemic ancestral clones and the secondary nature of microdeletions and RTK-RAS mutations. Leukemia. 2010;24(5):924-931.
12. Dobson SM, Garcia-Prat L, Vanner RJ, et al. Relapse-fated latent diagnosis subclones in acute B lineage leukemia are drug tolerant and possess distinct metabolic programs. Cancer Discov. 2020;10(4):568-587.
13. Kuster L, Grausenburger R, Fuka G, et al. ETV6/RUNX1-positive relapses evolve from an ancestral clone and frequently acquire deletions of genes implicated in glucocorticoid signaling. Blood. 2011;117(9):2658-2667.
14. Ma X, Edmonson M, Yergeau D, et al. Rise and fall of subclones from diagnosis to relapse in pediatric B-acute lymphoblastic leukaemia. Nat Commun. 2015;6:6604.
15. van Delft FW, Horsley S, Colman S, et al. Clonal origins of relapse in ETV6-RUNX1 acute lymphoblastic leukemia. Blood. 2011;117(23):6247-6254.
16. Yang JJ, Bhojwani D, Yang W, et al. Genome-wide copy number profiling reveals molecular evolution from diagnosis to relapse in childhood acute lymphoblastic leukemia. Blood. 2008;112(10):4178-4183.
17. Irving J, Matheson E, Minto L, et al. Ras pathway mutations are prevalent in relapsed childhood acute lymphoblastic leukemia and confer sensitivity to MEK inhibition. Blood. 2014;124(23):3420-3430.
18. Irving JA, Minto L, Bailey S, Hall AG. Loss of heterozygosity and somatic mutations of the glucocorticoid receptor gene are rarely found at relapse in pediatric acute lymphoblastic leukemia but may occur in a subpopulation early in the disease course. Cancer Res. 2005;65(21):9712-9718.
19. Campana D, Leung W. Clinical significance of minimal residual disease in patients with acute leukaemia undergoing haematopoietic stem cell transplantation. Br J Haematol. 2013;162(2):147-161.
20. Irving J, Jesson J, Virgo P, et al. Establishment and validation of a standard protocol for the detection of minimal residual disease in B lineage childhood acute lymphoblastic leukemia by flow cytometry in a multi-center setting. Haematologica. 2009;94(6):870-874.
21. Dixon ZA, Nicholson L, Zeppetzauer M, et al. CREBBP knockdown enhances RAS/RAF/MEK/ERK signaling in Ras pathway mutated acute lymphoblastic leukemia but does not modulate chemotherapeutic response. Haematologica. 2017;102(4):736-745.
22. Steeghs EMP, Jerchel IS, de Goffau-Nobel W, et al. JAK2 aberrations in childhood B-cell precursor acute lymphoblastic leukemia. Oncotarget. 2017;8(52):89923-89938.
23. Tasian SK, Teachey DT, Li Y, et al. Potent efficacy of combined PI3K/mTOR and JAK or ABL inhibition in murine xenograft models of Ph-like acute lymphoblastic leukemia. Blood. 2017;129(2):177-187.
24. Hao Q, Dai C, Deng Y, et al. Pooling analysis on prognostic value of PHH3 expression in cancer patients. Cancer Manag Res. 2018;10:2279-2288.
25. Perez-Cadahia B, Drobic B, Davie JR. H3 phosphorylation: dual role in mitosis and interphase. Biochem Cell Biol. 2009;87(5):695-709.
26. Ebinger S, Ozdemir EZ, Ziegenhain C, et al. Characterization of rare, dormant, and therapy-resistant cells in acute lymphoblastic leukemia. Cancer Cell. 2016;30(6):849-862.
27. Sarno J, Savino AM, Buracchi C, et al. SRC/ABL inhibition disrupts CRLF2-driven signaling to induce cell death in B-cell acute lymphoblastic leukemia. Oncotarget. 2018;9(33):22872-22885.
28. Pigazzi M, Ricotti E, Germano G, Faggian D, Arico M, Basso G. cAMP response element binding protein (CREB) overexpression CREB has been described as critical for leukemia progression. Haematologica. 2007;92(10):1435-1437.
29. Shabestari RM, Safa M, Alikarami F, Banan M, Kazemi A. CREB knockdown inhibits growth and induces apoptosis in human pre-B acute lymphoblastic leukemia cells through inhibition of prosurvival signals. Biomed Pharmacother. 2017;87:274-279.
30. van der Sligte NE, Kampen KR, ter Elst A, et al. Essential role for cyclic-AMP responsive element binding protein 1 (CREB) in the survival of acute lymphoblastic leukemia. Oncotarget. 2015;6(17):14970-14981.
31. Good Z, Sarno J, Jager A, et al. Single-cell developmental classification of B cell precursor acute lymphoblastic leukemia at diagnosis reveals predictors of relapse. Nat Med. 2018;24(4):474-483.
32. Kimura K, Ikoma A, Shibakawa M, et al. Safety, tolerability, and preliminary efficacy of the anti-fibrotic small molecule PRI-724, a CBP/beta-catenin inhibitor, in patients with hepatitis C virus-related cirrhosis: a single-center, open-label, dose escalation phase 1 trial. EBioMedicine. 2017;23:79-87.
33. Li BX, Gardner R, Xue C, et al. Systemic inhibition of CREB is well-tolerated in vivo. Sci Rep. 2016;6:34513.
34. Xie F, Li BX, Kassenbrock A, et al. Identification of a potent inhibitor of CREB-mediated gene transcription with efficacious in vivo anticancer activity. J Med Chem. 2015;58(12):5075-5087.